EUROPEAN ORGANIZATION FOR NUCLEAR RESEARCH

CERN-PPE/96-43
March 19, 1996

Studies of QCD in $e^+e^- \to$ Hadrons at $E_{cm} = 130$ and 136 GeV

The ALEPH Collaboration

Abstract

An analysis of the properties of hadronic final states produced in electron-positron annihilation at centre-of-mass energies of 130 and 136 GeV is presented. The measurements are based on a data sample of 5.7 pb^{-1} collected in November 1995 with the ALEPH detector at LEP. Inclusive charged particle distributions, jet rates and event-shape distributions are measured and the results are compared with the predictions of QCD-based models. From the measured distributions quantities are determined for which the dependence on the centre-of-mass energy can be predicted by QCD, including the mean multiplicity of charged particles, the peak position of the inclusive distribution of $\xi = -\ln x_p$ ($x_p = p/p_{beam}$), and the strong coupling constant α_s. The QCD predictions are tested by comparing with corresponding measurements at $E_{cm} = 91.2$ GeV and at lower energies.

Submitted to Physics Letters B

The ALEPH Collaboration

D. Buskulic, I. De Bonis, D. Decamp, P. Ghez, C. Goy, J.-P. Lees, A. Lucotte, M.-N. Minard, P. Odier, B. Pietrzyk

Laboratoire de Physique des Particules (LAPP), IN^{2}P^3-CNRS, 74019 Annecy-le-Vieux Cedex, France

M.P. Casado, M. Chmeissani, J.M. Crespo, M. Delfino,[12] I. Efthymiopoulos,[20] E. Fernandez, M. Fernandez-Bosman, Ll. Garrido,[15] A. Juste, M. Martinez, S. Orteu, A. Pacheco, C. Padilla, A. Pascual, J.A. Perlas, I. Riu, F. Sanchez, F. Teubert

Institut de Fisica d'Altes Energies, Universitat Autonoma de Barcelona, 08193 Bellaterra (Barcelona), Spain[7]

A. Colaleo, D. Creanza, M. de Palma, G. Gelao, M. Girone, G. Iaselli, G. Maggi,[3] M. Maggi, N. Marinelli, S. Nuzzo, A. Ranieri, G. Raso, F. Ruggieri, G. Selvaggi, L. Silvestris, P. Tempesta, G. Zito

Dipartimento di Fisica, INFN Sezione di Bari, 70126 Bari, Italy

X. Huang, J. Lin, Q. Ouyang, T. Wang, Y. Xie, R. Xu, S. Xue, J. Zhang, L. Zhang, W. Zhao

Institute of High-Energy Physics, Academia Sinica, Beijing, The People's Republic of China[8]

R. Alemany, A.O. Bazarko, M. Cattaneo, P. Comas, P. Coyle, H. Drevermann, R.W. Forty, M. Frank, R. Hagelberg, J. Harvey, P. Janot, B. Jost, E. Kneringer, J. Knobloch, I. Lehraus, G. Lutters, E.B. Martin, P. Mato, A. Minten, R. Miquel, Ll.M. Mir,[2] L. Moneta, T. Oest,[1] J.-F. Pusztaszeri, F. Ranjard, P. Rensing,[31] L. Rolandi, D. Schlatter, M. Schmelling,[24] O. Schneider, W. Tejessy, I.R. Tomalin, A. Venturi, H. Wachsmuth, A. Wagner

European Laboratory for Particle Physics (CERN), 1211 Geneva 23, Switzerland

Z. Ajaltouni, A. Barrès, C. Boyer, A. Falvard, P. Gay, C . Guicheney, P. Henrard, J. Jousset, B. Michel, S. Monteil, J-C. Montret, D. Pallin, P. Perret, F. Podlyski, J. Proriol, J.-M. Rossignol

Laboratoire de Physique Corpusculaire, Université Blaise Pascal, IN^{2}P^3-CNRS, Clermont-Ferrand, 63177 Aubière, France

T. Fearnley, J.B. Hansen, J.D. Hansen, J.R. Hansen, P.H. Hansen, B.S. Nilsson, A. Wäänänen

Niels Bohr Institute, 2100 Copenhagen, Denmark[9]

A. Kyriakis, C. Markou, E. Simopoulou, I. Siotis, A. Vayaki, K. Zachariadou

Nuclear Research Center Demokritos (NRCD), Athens, Greece

A. Blondel, J.C. Brient, A. Rougé, M. Rumpf, A. Valassi,[6] H. Videau[21]

Laboratoire de Physique Nucléaire et des Hautes Energies, Ecole Polytechnique, IN^{2}P^3-CNRS, 91128 Palaiseau Cedex, France

E. Focardi,[21] G. Parrini

Dipartimento di Fisica, Università di Firenze, INFN Sezione di Firenze, 50125 Firenze, Italy

M. Corden, C. Georgiopoulos, D.E. Jaffe

Supercomputer Computations Research Institute, Florida State University, Tallahassee, FL 32306-4052, USA [13,14]

A. Antonelli, G. Bencivenni, G. Bologna,[4] F. Bossi, P. Campana, G. Capon, D. Casper, V. Chiarella, G. Felici, P. Laurelli, G. Mannocchi,[5] F. Murtas, G.P. Murtas, L. Passalacqua, M. Pepe-Altarelli

Laboratori Nazionali dell'INFN (LNF-INFN), 00044 Frascati, Italy

L. Curtis, S.J. Dorris, A.W. Halley, I.G. Knowles, J.G. Lynch, V. O'Shea, C. Raine, P. Reeves, J.M. Scarr, K. Smith, A.S. Thompson, F. Thomson, S. Thorn, R.M. Turnbull

Department of Physics and Astronomy, University of Glasgow, Glasgow G12 8QQ,United Kingdom[10]

U. Becker, C. Geweniger, G. Graefe, P. Hanke, G. Hansper, V. Hepp, E.E. Kluge, A. Putzer, B. Rensch, M. Schmidt, J. Sommer, H. Stenzel, K. Tittel, S. Werner, M. Wunsch

Institut für Hochenergiephysik, Universität Heidelberg, 69120 Heidelberg, Fed. Rep. of Germany[16]

D. Abbaneo, R. Beuselinck, D.M. Binnie, W. Cameron, P.J. Dornan, A. Moutoussi, J. Nash, J.K. Sedgbeer, A.M. Stacey, M.D. Williams

Department of Physics, Imperial College, London SW7 2BZ, United Kingdom[10]

G. Dissertori, P. Girtler, D. Kuhn, G. Rudolph

Institut für Experimentalphysik, Universität Innsbruck, 6020 Innsbruck, Austria[18]

A.P. Betteridge, C.K. Bowdery, P. Colrain, G. Crawford, A.J. Finch, F. Foster, G. Hughes, T. Sloan, E.P. Whelan, M.I. Williams

Department of Physics, University of Lancaster, Lancaster LA1 4YB, United Kingdom[10]

A. Galla, A.M. Greene, C. Hoffmann, K. Kleinknecht, G. Quast, B. Renk, E. Rohne, H.-G. Sander, P. van Gemmeren C. Zeitnitz

Institut für Physik, Universität Mainz, 55099 Mainz, Fed. Rep. of Germany[16]

J.J. Aubert,[21] A.M. Bencheikh, C. Benchouk, A. Bonissent,[21] G. Bujosa, D. Calvet, J. Carr, C. Diaconu, N. Konstantinidis, P. Payre, D. Rousseau, M. Talby, A. Sadouki, M. Thulasidas, A. Tilquin, K. Trabelsi

Centre de Physique des Particules, Faculté des Sciences de Luminy, IN^{2}P^3-CNRS, 13288 Marseille, France

M. Aleppo, F. Ragusa[21]

Dipartimento di Fisica, Universitá di Milano e INFN Sezione di Milano, 20133 Milano, Italy.

I. Abt, R. Assmann, C. Bauer, W. Blum, H. Dietl, F. Dydak,[21] G. Ganis, C. Gotzhein, K. Jakobs, H. Kroha, G. Lütjens, G. Lutz, W. Männer, H.-G. Moser, R. Richter, A. Rosado-Schlosser, S. Schael, R. Settles, H. Seywerd, R. St. Denis, W. Wiedenmann, G. Wolf

Max-Planck-Institut für Physik, Werner-Heisenberg-Institut, 80805 München, Fed. Rep. of Germany[16]

J. Boucrot, O. Callot, A. Cordier, M. Davier, L. Duflot, J.-F. Grivaz, Ph. Heusse, A. Höcker, M. Jacquet, D.W. Kim,[19] F. Le Diberder, J. Lefrançois, A.-M. Lutz, I. Nikolic, H.J. Park,[19] I.C. Park,[19] M.-H. Schune, S. Simion, J.-J. Veillet, I. Videau, D. Zerwas

Laboratoire de l'Accélérateur Linéaire, Université de Paris-Sud, IN^{2}P^3-CNRS, 91405 Orsay Cedex, France

P. Azzurri, G. Bagliesi, G. Batignani, S. Bettarini, C. Bozzi, G. Calderini, M. Carpinelli, M.A. Ciocci, V. Ciulli, R. Dell'Orso, R. Fantechi, I. Ferrante, A. Giassi, A. Gregorio, F. Ligabue, A. Lusiani, P.S. Marrocchesi, A. Messineo, F. Palla, G. Rizzo, G. Sanguinetti, A. Sciabà, P. Spagnolo, J. Steinberger, R. Tenchini, G. Tonelli,[26] C. Vannini, P.G. Verdini, J. Walsh

Dipartimento di Fisica dell'Università, INFN Sezione di Pisa, e Scuola Normale Superiore, 56010 Pisa, Italy

G.A. Blair, L.M. Bryant, F. Cerutti, J.T. Chambers, Y. Gao, M.G. Green, T. Medcalf, P. Perrodo, J.A. Strong, J.H. von Wimmersperg-Toeller

Department of Physics, Royal Holloway & Bedford New College, University of London, Surrey TW20 OEX, United Kingdom[10]

D.R. Botterill, R.W. Clifft, T.R. Edgecock, S. Haywood, P. Maley, P.R. Norton, J.C. Thompson, A.E. Wright

Particle Physics Dept., Rutherford Appleton Laboratory, Chilton, Didcot, Oxon OX11 OQX, United Kingdom[10]

B. Bloch-Devaux, P. Colas, S. Emery, W. Kozanecki, E. Lançon, M.C. Lemaire, E. Locci, B. Marx, P. Perez, J. Rander, J.-F. Renardy, A. Roussarie, J.-P. Schuller, J. Schwindling, A. Trabelsi, B. Vallage

CEA, DAPNIA/Service de Physique des Particules, CE-Saclay, 91191 Gif-sur-Yvette Cedex, France[17]

S.N. Black, J.H. Dann, R.P. Johnson, H.Y. Kim, A.M. Litke, M.A. McNeil, G. Taylor

Institute for Particle Physics, University of California at Santa Cruz, Santa Cruz, CA 95064, USA[22]

C.N. Booth, R. Boswell, C.A.J. Brew, S. Cartwright, F. Combley, A. Koksal, M. Letho, W.M. Newton, J. Reeve, L.F. Thompson

Department of Physics, University of Sheffield, Sheffield S3 7RH, United Kingdom[10]

A. Böhrer, S. Brandt, V. Büscher, G. Cowan, C. Grupen, P. Saraiva, L. Smolik, F. Stephan,

Fachbereich Physik, Universität Siegen, 57068 Siegen, Fed. Rep. of Germany[16]

M. Apollonio, L. Bosisio, R. Della Marina, G. Giannini, B. Gobbo, G. Musolino

Dipartimento di Fisica, Università di Trieste e INFN Sezione di Trieste, 34127 Trieste, Italy

J. Putz, J. Rothberg, S. Wasserbaech, R.W. Williams

Experimental Elementary Particle Physics, University of Washington, WA 98195 Seattle, U.S.A.

S.R. Armstrong, L. Bellantoni,[23] P. Elmer, Z. Feng,[28] D.P.S. Ferguson, Y.S. Gao,[29] S. González, J. Grahl, T.C. Greening, J.L. Harton,[27] O.J. Hayes, H. Hu, P.A. McNamara III, J.M. Nachtman, W. Orejudos, Y.B. Pan, Y. Saadi, M. Schmitt, I.J. Scott, V. Sharma,[25] A.M. Walsh,[30] Sau Lan Wu, X. Wu, J.M. Yamartino, M. Zheng, G. Zobernig

Department of Physics, University of Wisconsin, Madison, WI 53706, USA[11]

[1] Now at DESY, Hamburg, Germany.
[2] Supported by Dirección General de Investigación Científica y Técnica, Spain.
[3] Now at Dipartimento di Fisica, Università di Lecce, 73100 Lecce, Italy.
[4] Also Istituto di Fisica Generale, Università di Torino, Torino, Italy.
[5] Also Istituto di Cosmo-Geofisica del C.N.R., Torino, Italy.
[6] Supported by the Commission of the European Communities, contract ERBCHBICT941234.
[7] Supported by CICYT, Spain.
[8] Supported by the National Science Foundation of China.
[9] Supported by the Danish Natural Science Research Council.
[10] Supported by the UK Particle Physics and Astronomy Research Council.
[11] Supported by the US Department of Energy, grant DE-FG0295-ER40896.
[12] Also at Supercomputations Research Institute, Florida State University, Tallahassee, U.S.A.
[13] Supported by the US Department of Energy, contract DE-FG05-92ER40742.
[14] Supported by the US Department of Energy, contract DE-FC05-85ER250000.
[15] Permanent address: Universitat de Barcelona, 08208 Barcelona, Spain.
[16] Supported by the Bundesministerium für Forschung und Technologie, Fed. Rep. of Germany.
[17] Supported by the Direction des Sciences de la Matière, C.E.A.
[18] Supported by Fonds zur Förderung der wissenschaftlichen Forschung, Austria.
[19] Permanent address: Kangnung National University, Kangnung, Korea.
[20] Now at CERN, 1211 Geneva 23, Switzerland.
[21] Also at CERN, 1211 Geneva 23, Switzerland.
[22] Supported by the US Department of Energy, grant DE-FG03-92ER40689.
[23] Now at Fermi National Accelerator Laboratory, Batavia, IL 60510, USA.
[24] Now at Max-Plank-Institüt für Kernphysik, Heidelberg, Germany.
[25] Now at University of California at San Diego, La Jolla, CA 92093, USA.
[26] Also at Istituto di Matematica e Fisica, Università di Sassari, Sassari, Italy.
[27] Now at Colorado State University, Fort Collins, CO 80523, USA.
[28] Now at The Johns Hopkins University, Baltimore, MD 21218, U.S.A.
[29] Now at Harvard University, Cambridge, MA 02138, U.S.A.
[30] Now at Rutgers University, Piscataway, NJ 08855-0849, U.S.A.
[31] Now at Dragon Systems, Newton, MA 02160, U.S.A.

1 Introduction

After running since the autumn of 1989 at centre-of-mass energies near the Z resonance, the energy of the LEP storage ring was increased in November 1995 to 130 and then to 136 GeV. Here an analysis of hadronic final states is presented based on approximately 2.9 pb^{-1} integrated luminosity collected by the ALEPH detector at each of these energies. The primary goal of the measurements is to investigate quantities for which the dependence on the centre-of-mass energy E_{cm} can be predicted by Quantum Chromodynamics. By comparing with corresponding measurements at $E_{cm} = M_Z$ and also with measurements from lower energy $\mathrm{e^+e^-}$ experiments, the predictions can be tested. A further goal of the measurements is to provide a check of QCD-based models of hadronic final states, which are used in many other investigations for purposes of estimating efficiencies and background, e.g. in searches for new particles and measurements of quantities related to electroweak physics.

Although it is not possible using perturbative QCD to calculate infrared sensitive quantities such as inclusive particle distributions, the E_{cm} dependence can be predicted once the distributions have been determined at a single energy. Infrared finite quantities such as jet rates and event-shape distributions can be computed perturbatively as a function of the running coupling $\alpha_s(E_{cm})$. In both cases the energy dependence is precisely specified. The predicted E_{cm} evolution of various quantities has been tested by comparisons of measurements at the Z resonance with those from lower energy $\mathrm{e^+e^-}$ machines. By going to higher energies, the E_{cm} dependence can be checked further in a regime where non-perturbative effects are expected to decrease. In this paper, measurements of the mean multiplicity of charged particles N_{ch}, the peak position $\xi^\star$ of the inclusive charged particle distribution of $\xi = -\ln x_p$ ($x_p = p/p_{beam}$), and the strong coupling constant α_s are presented.

2 Event Selection

Hadronic final states at c.m.s. energies higher than the Z resonance are characterized by a relatively high probability for initial state photon radiation (ISR) resulting in a hadronic system with an invariant mass of $\sqrt{s'} \approx M_Z$. Since the goal of the present analysis is to study hadronic systems produced with $\sqrt{s'} \approx E_{cm}$, cuts must be applied to suppress radiative events as completely as possible. This is particularly important in studies of global event properties, since the hadronic system is boosted away from the ISR photon(s) and typically results in two jets with an opening angle significantly less than 180°. Such an event structure mimics the effects of hard gluon radiation, and unless it is properly taken into account it would lead to an artificially high estimation of α_s.

A detailed description of the ALEPH detector is given in Ref. [1]. The measurements presented here are based on both charged particle measurements from the time projection chamber, inner tracking chamber, and vertex detector, as well as information on charged and neutral particles from the electromagnetic and hadronic calorimeters. An energy-flow reconstruction algorithm is applied, which takes advantage of the redundancy of energy and momentum measurements and exploits photon, electron and muon identification [2]. The output of this algorithm is a list of "energy-flow objects," with measured momentum vectors and information on particle type.

In a preliminary step, events are accepted if they have at least 7 charged particle tracks and if their total energy (assuming the pion mass) is at least 10% of E_{cm}. In order to ensure that the event is well contained within the detector, the polar angle of the sphericity axis is required to satisfy $|\cos\theta_{spher}| < 0.9$. After these cuts, samples of 727 and 586 events are obtained at 130 and 136 GeV, respectively.

ISR photons are most frequently emitted at very low angles and escape detection, in which case the visible mass of the event is reduced and the sum of the z components (z parallel to the beam) of the measured particle momenta is not equal to zero. Such events are easily removed by applying cuts on the

visible mass and p_z-sum. Not infrequently, however, the ISR photon(s) are detected, and special cuts must be applied to eliminate such events. This is done by first identifying ISR photons and removing them from the event. The p_z-sum and invariant mass of the remaining system are then examined to see if it resembles the hadronic decay of a Z, in which case the event is rejected.

More precisely, particles are tagged as ISR-photon candidates if they are detected at $|\cos\theta| > 0.988$, i.e. in the luminosity monitors LCAL or SICAL, regardless of their energy. For the case of a single ISR photon recoiling against an on-shell Z, the photon energy is given by $E_\gamma = (E_{cm}^2 - M_Z^2)/2E_{cm} = 33.0$ (37.4) GeV at $E_{cm} = 130$ (136) GeV. This is, in fact, the dominant case, and therefore photons are tagged as ISR if $E_\gamma > 20$ GeV regardless of their angle.

ISR photons are also emitted with lower energies, in which case they are considerably more difficult to identify as such. Monte Carlo studies indicate that they are isolated from the hadrons in the event, and therefore photons with energies between 5 and 20 GeV are tagged as ISR if the smallest invariant mass of the photon with a charged particle is at least 1.5 GeV. No attempt is made to tag ISR photons with energies below 5 GeV.

ISR photons emitted at low angles traverse a larger than average amount of detector material, and the probability for pair conversion is thus increased. In order to find conversion pairs, electron and positron candidates are first selected using information on the shower shape in the electromagnetic calorimeter and the ionization rate ($\mathrm{d}E/\mathrm{d}x$) measured in the TPC [2]. To be identified as a photon, an $\mathrm{e^+e^-}$ pair is required to have an invariant mass less than 50 MeV (determined at the conversion point) and the $\mathrm{e^+e^-}$ trajectories must fulfill radius dependent requirements of spatial separation. A photon conversion is tagged as ISR using the same criteria as for photons reconstructed in the electromagnetic calorimeter.

After having identified and removed ISR-candidate particles according to the cuts described above, the remaining part of the event is used to compute the visible mass M_{vis} and the absolute value of the p_z-sum. Non-radiative events are characterized by a high M_{vis} and low $|\sum p_z|$, and the difference of the two quantities

$$\Delta = M_{vis} - |\sum p_z| \tag{1}$$

is found to be a sensitive indicator of the true mass of the hadronic system $\sqrt{s'}$. Distributions of Δ for $E_{cm} = 130$ and 136 GeV along with the predictions from the PYTHIA Monte Carlo model (version 5.7 [4]) plus full detector simulation are shown in Fig. 1.

Hadronic events were then selected by requiring $\Delta > 100$ GeV (for both c.m.s. energies). The measurements of the various distributions use all particles of the accepted events, including those which had previously been tagged as ISR photons. The numbers of selected events and estimates based on Monte Carlo simulations of the event selection efficiencies, the fraction of radiative events, and the mean values of the true mass of the hadronic system $\sqrt{s'}$ are shown in Table 1.

E_{cm} (GeV)	events accepted	efficiency for $\sqrt{s'} \geq 0.9E_{cm}$	impurity ($\sqrt{s'} < 100$ GeV)	$\langle\sqrt{s'}\rangle$ (GeV)
130	163	69.2%	2.4%	126.4
136	136	72.5%	3.0%	131.4

Table 1: Centre-of-mass energy E_{cm}, number of selected events, selection efficiency for events with a true hadronic mass approximately equal to E_{cm}, impurity, defined as the fraction of selected events with $\sqrt{s'} < 100$ GeV, and mean value of the true hadronic mass $\sqrt{s'}$.

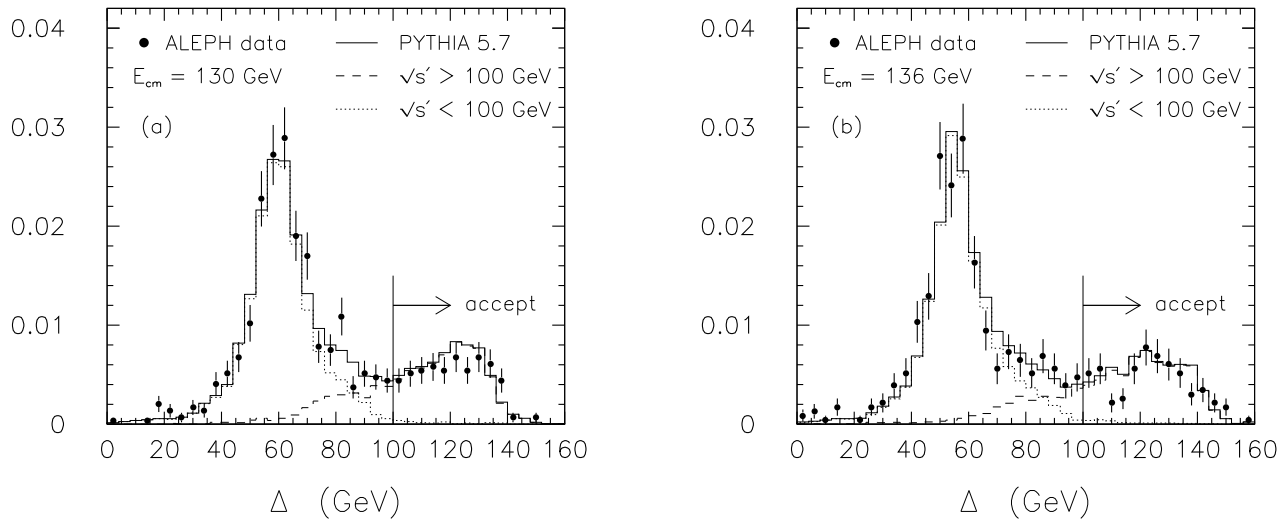

Figure 1: Distributions normalized to unit area of $\Delta = M_{vis} - |\sum p_z|$ for (a) $E_{cm} = 130$ GeV and (b) $E_{cm} = 136$ GeV along with the predictions of the PYTHIA model including full detector simulation. The dashed (dotted) distributions show the components for which the true hadronic mass is greater (less) than 100 GeV.

3 Corrections for Detector Effects and Estimation of Systematic Errors

The measured distributions were corrected for effects of geometrical acceptance, detector efficiency and resolution, decays, particle interactions with the material of the detector, effects of event and track selection, as well as the residual effects of initial state photon radiation. This was done by means of bin-by-bin multiplicative correction factors C, relating the measured value of a quantity X to its corrected value,

$$X_{corrected} = X_{measured} \cdot C \ . \tag{2}$$

The correction factors are computed using the same procedure as in Ref. [3],

$$C = \frac{X_{generator}}{X_{MC+det.\,sim.}} \ . \tag{3}$$

Here $X_{generator}$ is computed using the generator only (no detector simulation) with ISR turned off, with all particles having mean lifetimes less than 10^{-9} seconds required to decay, and all others treated as stable. $X_{MC+det.\,sim.}$ is computed from fully simulated and reconstructed Monte Carlo data based on PYTHIA 5.7 (10000 events at both 130 and 136 GeV).

In a first step, the data at 130 and 136 GeV were treated separately, and it was checked that at both energies the data were in good agreement with Monte Carlo predictions. In order to present only a single final set of distributions, however, the data sets were combined by correcting them both to $E_{cm} = 133$ GeV and then averaging the result. The correction to 133 GeV is done by computing $X_{generator}$ in the correction factors Eq. (3) with $E_{cm} = 133$ GeV, whereas $X_{MC+det.\,sim.}$ is computed with the same E_{cm} as that of the real data.

Although the bin-by-bin correction procedure is to a good approximation independent of the event generator used, a small dependence remains and must be taken into account when estimating systematic errors. For this purpose, samples of 10000 events at both 130 and 136 GeV were generated with the HERWIG model version 5.8d [5], including simulation of initial state radiation. Since studies at LEP I have indicated that JETSET provides a better description of the data than HERWIG, the final distributions are computed with the PYTHIA based corrections. (For the process $e^+e^- \to$ *hadrons* PYTHIA and the JETSET parton shower model [4] can be regarded as essentially equivalent. PYTHIA is used here because of its better modelling of initial state radiation.) The difference between distributions corrected using PYTHIA and HERWIG is included in the systematic errors.

In order to test the sensitivity of the final results to the event selection procedure, the analysis was repeated using an alternative scheme for identifying ISR photons. This was done by first constructing jets using the JADE clustering algorithm [6] with a jet resolution parameter of $y_{cut} = 0.008$. Jets were tagged as "electromagnetic" if their energy was at least 10 GeV, of which at least 80% was detected as photons either in the electromagnetic calorimeter or as e^+e^- conversion pairs. The photons from these jets were then removed, as were all clusters from the luminosity calorimeters. The quantity Δ was then determined and events were selected for which $\Delta > 95$ GeV. The changes in the corrected distributions with respect to those obtained using the standard event selection procedure are included in the systematic errors.

In addition, the sensitivity of the results to variations in the event selection cuts was investigated. The greatest sensitivity was found when varying the cut on Δ, although to a large extent the changes were compatible with those expected from statistical fluctuations (cf. Section 4 concerning N_{ch} and $\xi^\star$). The changes in the corrected values when moving the cut on Δ by ± 5 GeV are included in the systematic uncertainty.

The full systematic errors are taken as the quadratic sums of the components described above. The error bars on all of the plots are the quadratic sum of systematic and statistical uncertainties.

4 Inclusive Charged Particle Distributions

Charged particle inclusive distributions were measured for the variables $x_p = p/p_{beam}$, $\xi = -\ln x_p$, the rapidity $y = \frac{1}{2}\ln(E + p_\parallel)/(E - p_\parallel)$ with $p_\parallel$ measured with respect to the thrust axis, and the transverse momentum components in and out of the event plane defined by the sphericity tensor, $p_\perp^{in}$ and $p_\perp^{out}$. The thrust axis used for rapidity and the event plane used for $p_\perp^{in}$ and $p_\perp^{out}$ are determined using both charged and neutral particles.

Correction factors for the inclusive distributions are typically in the range $0.7 < C < 1.3$, with somewhat larger corrections near phase-space limits and at low rapidity (up to $C \approx 1.7$). The factors derived from PYTHIA are in good agreement with those from HERWIG.

Corrected inclusive distributions of x_p, y, $p_\perp^{in}$ and $p_\perp^{out}$ are shown in Fig. 2, along with the predictions of the PYTHIA, HERWIG and ARIADNE (version 4.06 [7]) models with initial state radiation turned off. The model parameters have been tuned using data from $E_{cm} = 91.2$ GeV [8] (see also [3]). The agreement between data and predictions is seen to be quite good.

The statistical errors for the inclusive distributions were computed so as to take into account the non-Poissonian nature of the number of entries per event in a given bin. That is, the error is taken as the standard deviation of the multiplicity per event in a given bin divided by the square root of the number of events. This was found to be particularly important for the rapidity distribution at low values of rapidity (cf. Ref. [9]). For example, the particles in a jet with a certain (large) angle with respect to the thrust axis all have approximately the same rapidity. Thus a single jet can contribute many entries in the same rapidity bin, so that comparatively rare events lead to a significant fraction of the total number of entries. In this case the statistical fluctuations are considerably larger ($\sim 60\%$) than what one would

have with a Poisson variable of the same mean. For about $y > 3$ and for the x_p, ξ and $p_\perp$ distributions, the errors are only slightly larger than what one would derive from Poisson statistics.

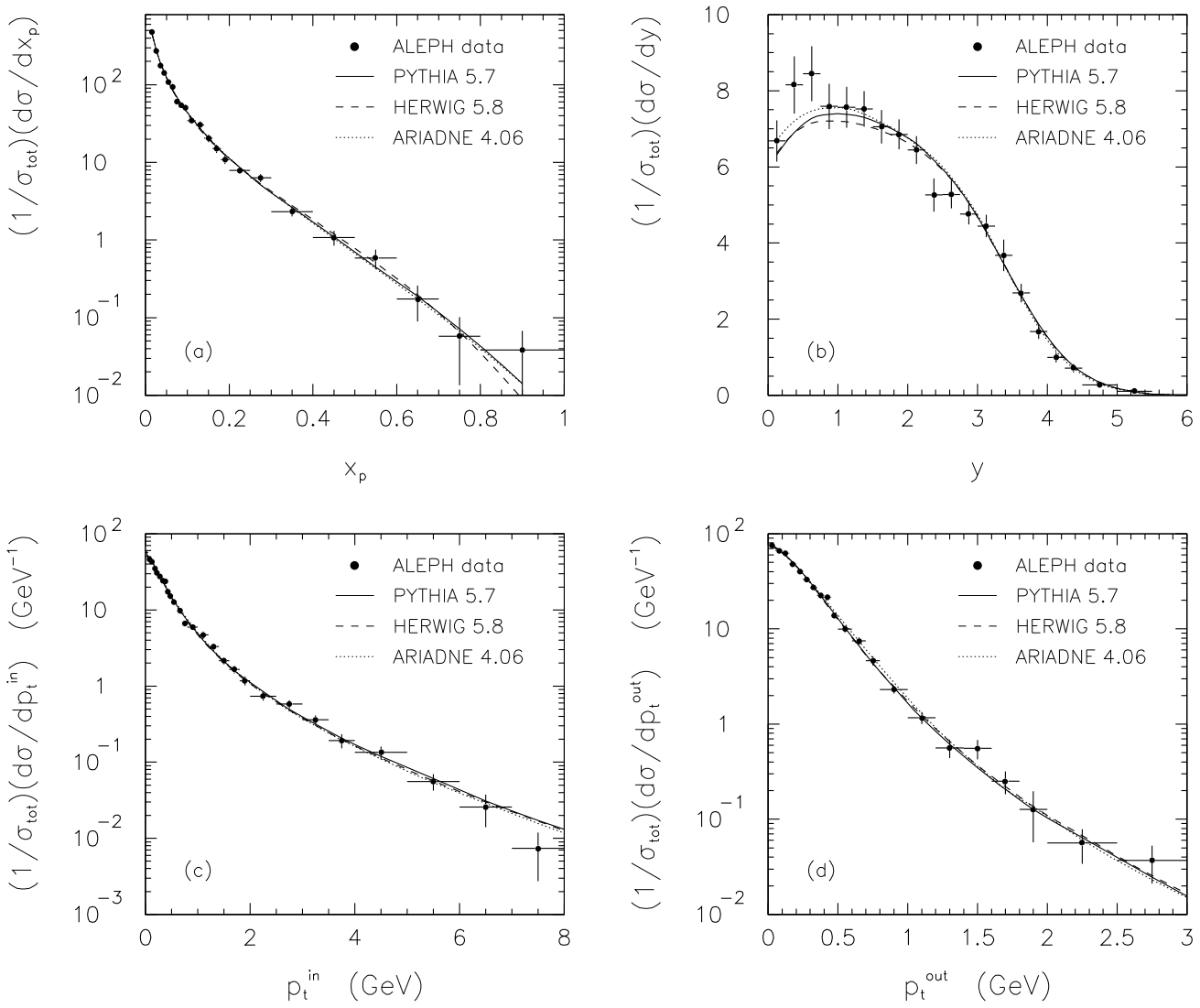

Figure 2: Inclusive charged particle distributions of (a) $x_p = p/p_{beam}$, (b) rapidity, (c) transverse momentum component in the event plane, (d) transverse momentum component out of the event plane.

From the integral of the rapidity distribution the mean multiplicity of charged particles can be determined. This was done separately at each c.m.s. energy, resulting in

$$N_{ch}(130\,\mathrm{GeV}) = 23.61 \pm 0.54\,(stat.) \pm 0.36\,(sys.)\,,$$

$$N_{ch}(136\,\mathrm{GeV}) = 25.01 \pm 0.70\,(stat.) \pm 0.36\,(sys.)\,.$$

The statistical error is obtained from the standard deviation of the multiplicity distribution divided by the square root of the number of events. The selection procedure based on the alternative scheme for tagging ISR photons leads to N_{ch} values differing by -0.11 $(+0.09)$ from the values given above for 130 (136) GeV. The generator dependence was also found to be small, with the differences in N_{ch} resulting

from PYTHIA and HERWIG based corrections differing by less than 0.1. Raising the cut on Δ from 100 to 105 GeV caused N_{ch} to increase by 0.47 at 130 and by 0.21 at 136 GeV. The average change of 0.34 is taken for this component of the error.

By carrying out the same procedure with the combined rapidity distribution corrected to 133 GeV, a mean multiplicity of

$$N_{ch}(133\,\mathrm{GeV}) = 24.15 \pm 0.43\,(stat.) \pm 0.34\,(sys.)$$

is obtained. This is in good agreement with the measurements by the DELPHI [10] and L3 [11] experiments.

The measured charged particle multiplicity at 133 GeV is shown in Fig. 3 along with measurements at lower c.m.s. energies [3, 12] as well as the predictions of several Monte Carlo models. Both PYTHIA and HERWIG are in reasonably good agreement with the data. The JETSET $O(\alpha_s^2)$ model does not predict a fast enough rise in N_{ch} for increasing E_{cm}. This confirms that multiple gluon emission, which is simulated in the parton shower approach but not in the matrix element model, is necessary to describe the energy dependence of N_{ch}.

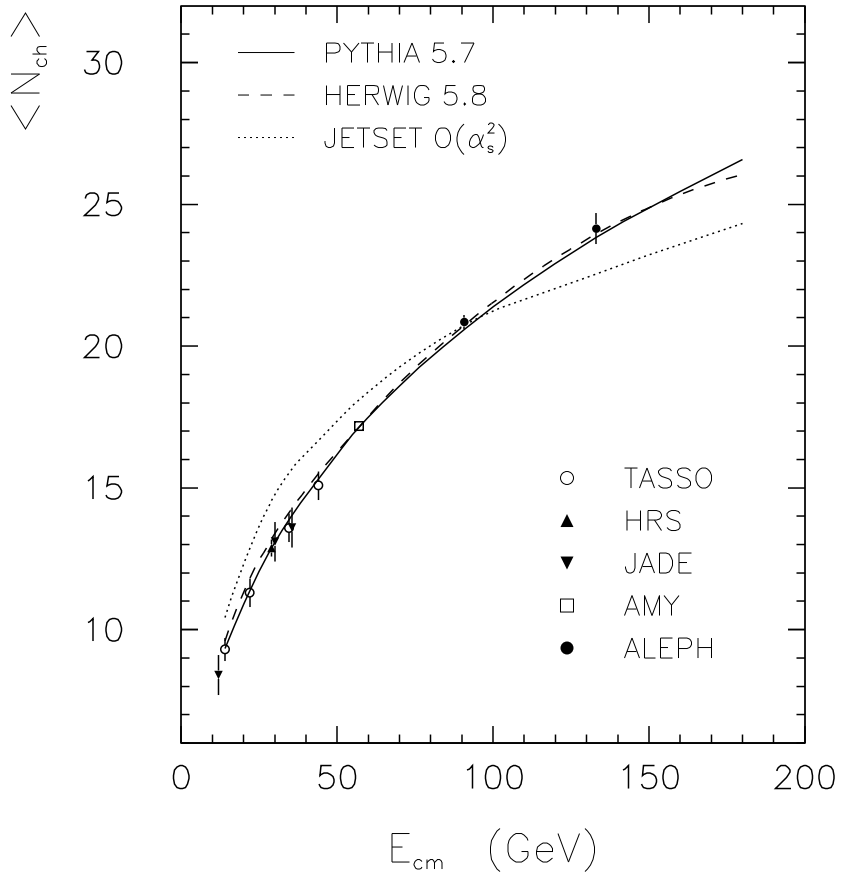

Figure 3: Mean multiplicity of charged particles versus E_{cm} as measured at various centre-of-mass energies, and the predictions of several Monte Carlo models.

By transforming to the variable $\xi = -\ln x_p$ the low momentum (high ξ) region is greatly expanded. The inclusive distribution of ξ for 130 and 136 GeV combined (corrected to $E_{cm} = 133$ GeV) is shown in Fig. 4a compared with the predictions of PYTHIA, HERWIG, and ARIADNE.

The peak position ξ^* can be determined by fitting a Gaussian to the central region of the distribution, chosen here to be $2.5 < \xi < 5.5$. This gives

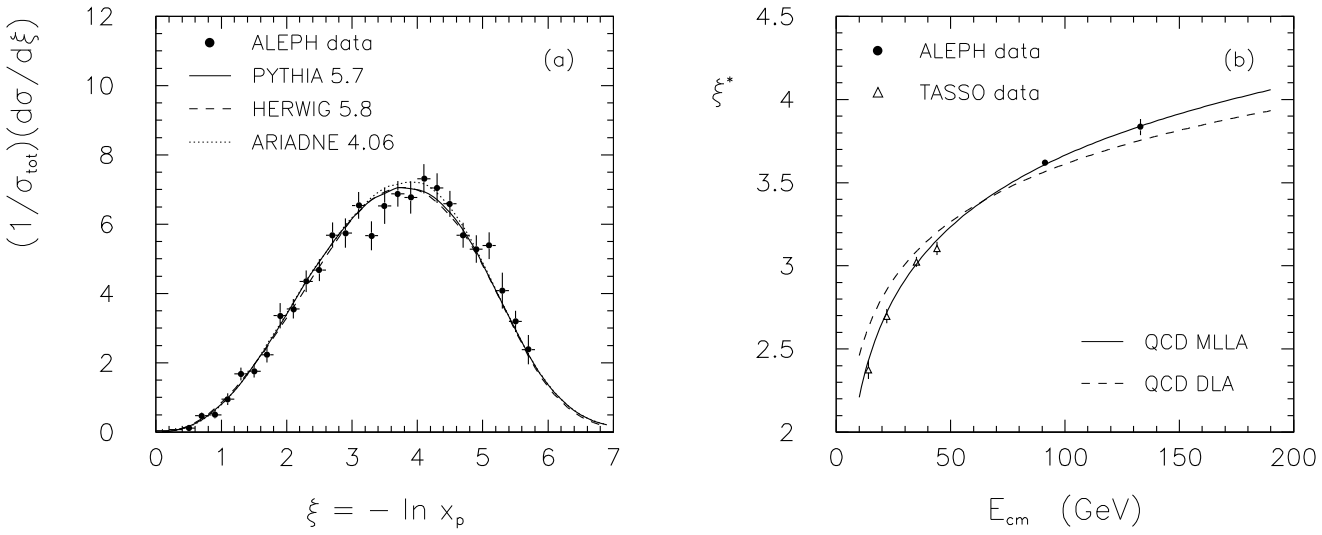

Figure 4: (a) The inclusive charged particle distribution of $\xi = -\ln x_p$. (b) The peak position of the ξ distribution as a function of centre-of-mass energy (see text).

$$\xi^*(130\,\mathrm{GeV}) = 3.746 \pm 0.051\,(stat.) \pm 0.043\,(sys.)\,,$$

$$\xi^*(136\,\mathrm{GeV}) = 3.975 \pm 0.062\,(stat.) \pm 0.043\,(sys.)\,,$$

where the systematic uncertainty was estimated by means of the same changes in the analysis procedure as described for N_{ch} above. By using the combined ξ distribution corrected to 133 GeV one obtains

$$\xi^*(133\,\mathrm{GeV}) = 3.834 \pm 0.038\,(stat.) \pm 0.029\,(sys.)\,.$$

The smaller systematic error at 133 GeV results from a partial cancelation of the change in ξ^* when the cut on Δ is increased by 5 GeV. This is $+0.038$ at 130 GeV and -0.014 at 136 GeV. The value of ξ^* determined here at 133 GeV as well as from ALEPH data at $E_{cm} = 91.2$ GeV [8] and from TASSO data [13] at $E_{cm} = 14$, 22, 35 and 44 GeV are shown in Fig. 4b. Also shown are the leading-order QCD prediction (DLA – Double Logarithmic Approximation) and the prediction including higher order corrections (MLLA – Modified Leading Log Approximation) [14]. One sees from Fig. 4b that the inclusion of higher order corrections moves the prediction into good overall agreement with the experimental data.

5 Event-Shape Variables and Jet Rates

Information on the global structure of hadronic events can be obtained from event-shape variables and jet-rates. Here the variables thrust T, differential two-jet rate y_3, and the n-jet rates for $n = 2, 3, 4, 5$ are considered. The measurements are based on both charged and neutral particles. The thrust of an event is defined as $T = \max(\sum_j |p_{\parallel j}| / \sum_j |p_j|)$ where the sum is over all the selected particles in the event. Jet rates and the variable y_3 are defined by means of the Durham clustering algorithm [16, 17] in the following way. For each pair of particles i and j in an event one computes

$$y_{ij} = \frac{2\min(E_i^2, E_j^2)(1-\cos\theta_{ij})}{E_{vis}^2} \,. \tag{4}$$

The pair of particles with the smallest value of y_{ij} is replaced by a pseudo-particle (cluster). The four-momentum of the cluster is taken to be the sum of the four momenta of particles i and j, $p^\mu = p_i^\mu + p_j^\mu$ ("E" recombination scheme). The clustering procedure is repeated until all y_{ij} values exceed a given threshold y_{cut}. The number of clusters remaining at this point is defined to be the number of jets. Alternatively, one can continue the algorithm until exactly three clusters remain. The smallest value of y_{ij} in this configuration is defined as y_3. In this way one obtains a single number for each event, whose distribution is sensitive to the probability of hard gluon radiation leading to a three-jet topology.

The detector correction factors are found to lie in the range $0.5 < C < 1.5$. Systematic uncertainties have been estimated by using the alternative event-selection procedure as described above, variation of experimental cuts, and by computing the detector correction factors with the HERWIG model. In all bins the statistical errors are larger than systematic, in most cases significantly so.

Figure 5 shows the corrected distributions of thrust T and $L = -\ln y_3$ along with the predictions of the PYTHIA, HERWIG, and ARIADNE models. The models and data are in reasonably good agreement, although there is an excess with respect to model predictions in the number of events at very low thrust.

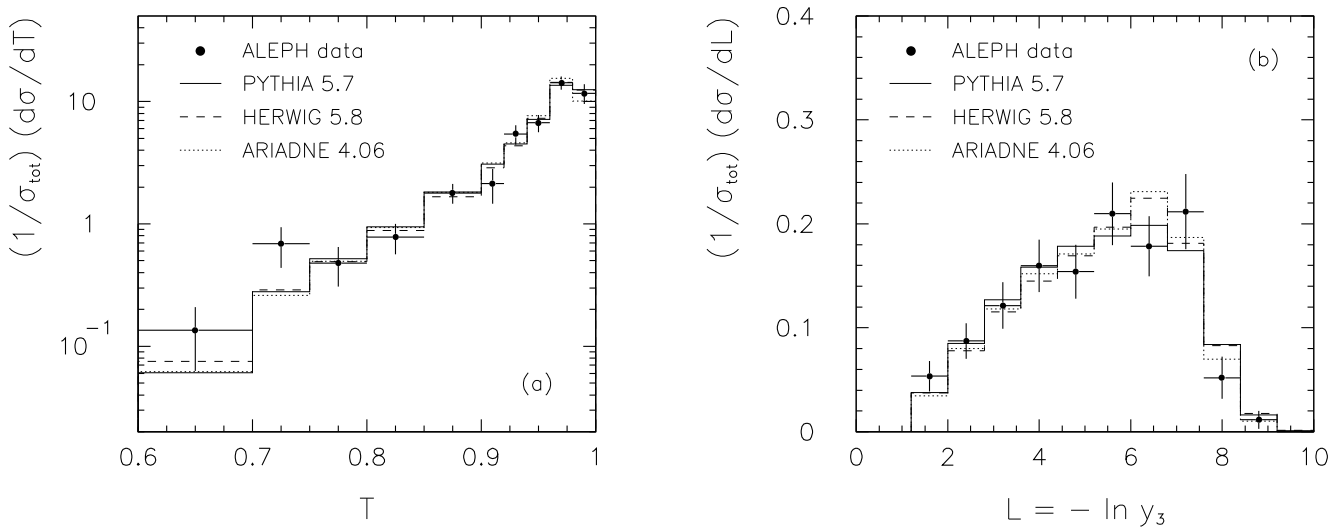

Figure 5: Distributions of (a) thrust and (b) $L = -\ln y_3$ at $E_{cm} = 133$ GeV with predictions of Monte Carlo models.

From the thrust distribution a mean value of

$$\langle 1 - T \rangle = 0.0666 \pm 0.0060\,(stat.) \pm 0.0030\,(sys.)$$

is obtained. This is shown in Fig. 6 along with measurements at other c.m.s. energies [3, 12, 13] and the predictions of Monte Carlo models.

The n-jet rates for $n = 2, 3, 4, 5$ were measured using the Durham algorithm as described above, and detector correction factors were applied in the same manner as for the event-shape distributions, but here for each value of the jet resolution parameter y_{cut}. Results are shown in Fig. 7 along with the predictions of PYTHIA and the JETSET $O(\alpha_s^2)$ matrix element model. The error bars are the quadratic sum of statistical and systematic uncertainties. The systematic errors, estimated using the same procedures as for the event-shape distributions, are always similar to or smaller than the statistical errors.

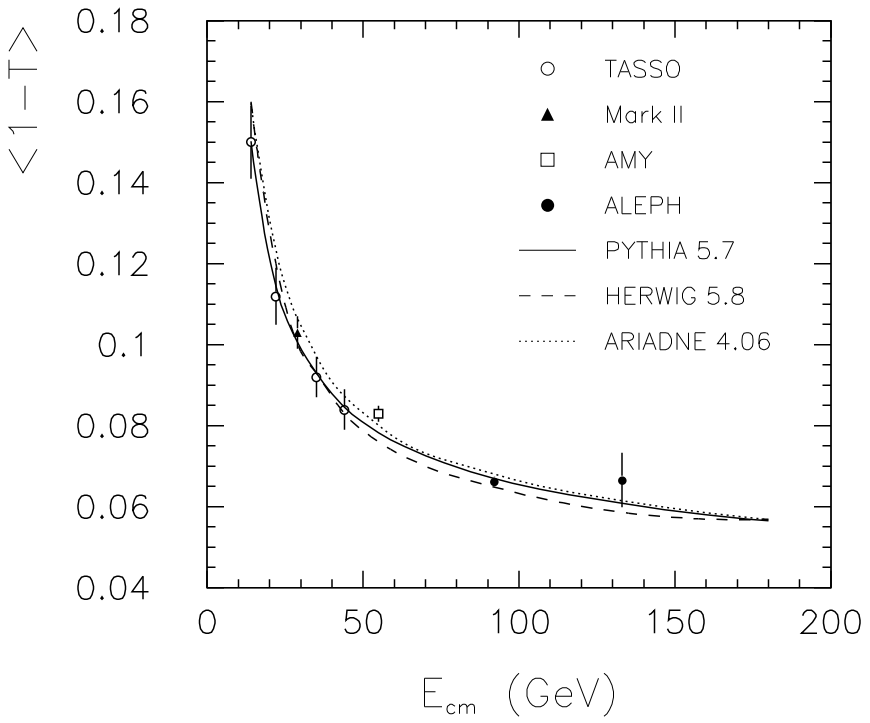

Figure 6: Mean value of $1-T$ versus E_{cm} as measured at various centre-of-mass energies, and the predictions of several Monte Carlo models.

The JETSET $O(\alpha_s^2)$ model is of particular interest for four-jet studies, because it contains the exact $O(\alpha_s^2)$ matrix element for four-parton final states. PYTHIA, on the other hand, uses a parton shower model based on the leading-logarithm approximation, supplemented by a matching of the three-jet rate to the $O(\alpha_s)$ matrix element. A disadvantage of the $O(\alpha_s^2)$ matrix-element model is that the mean particle multiplicity is poorly described when using model parameters tuned at $E_{cm} = 91.2$ GeV (cf. Fig. 3). In order to provide a more realistic test of the jet rates, the two parameters a and b of the Lund symmetric fragmentation function (see [4]) were adjusted from $a = 1.0$ to 1.1 and $b = 0.495\,\mathrm{GeV}^{-2}$ to $0.4\,\mathrm{GeV}^{-2}$ resulting in a mean charged particle multiplicity of $N_{ch} = 23.8$ at $E_{cm} = 133$ GeV, in approximate agreement with the data.

Despite the differences between the two models at parton level, the predicted four-jet rates are similar. The measured four-jet rate is observed to be lower than predicted at small values of the jet-resolution parameter y_{cut}, but is greater than predicted for $y_{cut} > 0.01$. A further analysis of four-jet events based on the same data sample will be given in a forthcoming paper [18]. As expected, the matrix element model is unable to predict the five-jet rate, because at $O(\alpha_s^2)$ a maximum of four final state partons can be described.

6 Determination of α_s

One of the most important predictions of QCD is the energy dependence (running) of the strong coupling constant α_s. Accurate measurements of α_s have been made from jet rates and event-shape variables using LEP I data at a centre-of-mass energy $E_{cm} = 91.2$ GeV. For example, the value measured by ALEPH using event-shape variables with resummed QCD predictions is $\alpha_s(M_Z) = 0.125 \pm 0.005$ [15]. Given this value at $E_{cm} = M_Z$, QCD predicts $\alpha_s(133\,\mathrm{GeV}) = 0.118$, i.e. a relative decrease of 6%. Although this decrease is comparable to the size of the uncertainty in α_s, a large part of the error is highly correlated between the two energy points. A check of the running predicted by QCD is therefore possible as long

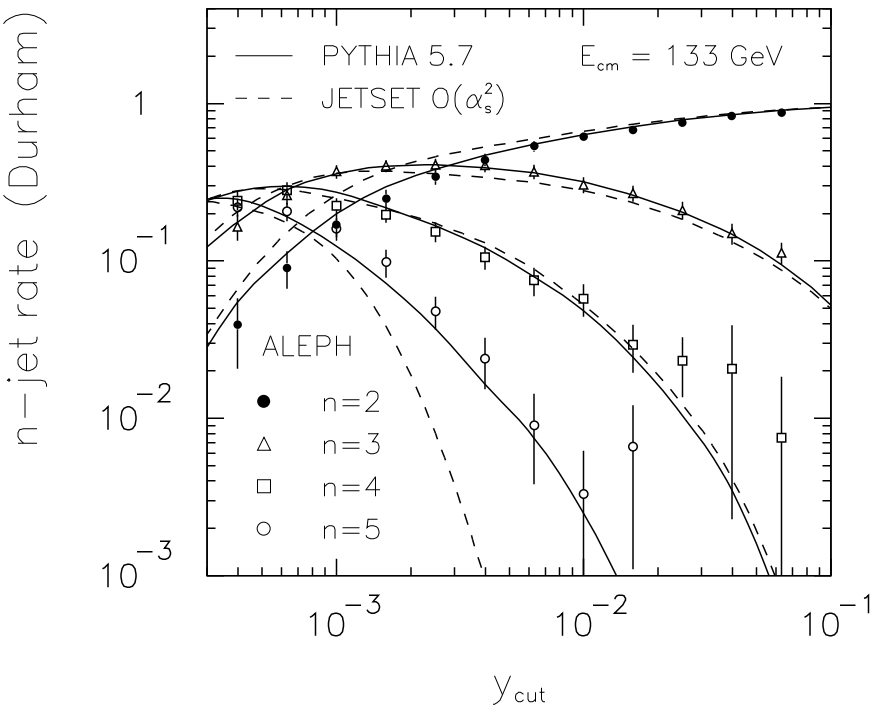

Figure 7: Measured n-jet rates for $n = 2, 3, 4, 5$ and the predictions of Monte Carlo models.

as the statistical and other uncorrelated components of the error are sufficiently small.

In order to obtain easily comparable measurements of α_s at both $E_{cm} = 91.2$ and 133 GeV, one would like to use the same variable and fit range for both energies. In this way, the theoretical errors from missing higher order terms in the perturbative prediction are expected to be approximately equal in both cases, which should allow a more accurate determination of the energy dependence.

In order to achieve a low statistical error at $E_{cm} = 133$ GeV it is necessary to use as large a fit range as possible, which must then include part of the region where collinear gluon emission is dominant. In this region, however, hadronization effects become important; these introduce an additional uncertainty into the measurement of α_s. Based on Monte Carlo studies and other theoretical considerations [19], the variable $L = -\ln y_3$ was found to have the smallest hadronization uncertainties over the largest range. In addition, the parton-level prediction is known to high accuracy owing to the recent calculation of higher order corrections [20]. The α_s measurement presented here is therefore based on the distribution of $-\ln y_3$.

Ratios of hadron to parton level distributions of $-\ln y_3$ from the models PYTHIA, HERWIG, and ARIADNE are shown in Fig. 8 for 91.2 and 133 GeV. As a compromise between reliable corrections and a small statistical error, the fit range was taken to be $1.2 < L < 7.6$.

The $-\ln y_3$ distribution measured at $E_{cm} = 91.2$ GeV has been published previously in Ref. [15] and used there to determine $\alpha_s(M_Z)$. The comparison here is based on an updated measurement done using approximately 110000 hadronic events from the 1992 running period. The analysis technique was essentially the same as that used for the 130 – 136 GeV data, although without the special cuts against events with initial state radiation.

Systematic errors for the 91.2 GeV measurement were estimated by variation of experimental cuts. In addition, the analysis was repeated as done in Ref. [15] with charged particles only, and then corrected so as to correspond to both charged and neutral particles. The various distributions from the alternative analysis methods were used to determine α_s and the resulting spread of values used to derive the

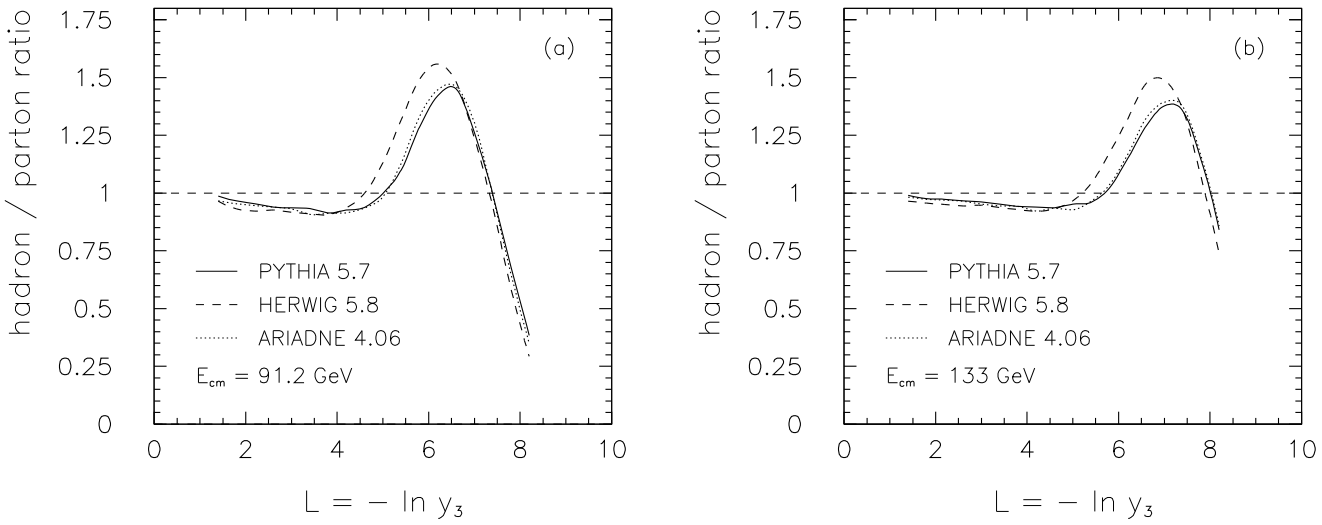

Figure 8: Ratios of hadron to parton level distributions of $L = -\ln y_3$ (a) at $E_{cm} = 91.2$ GeV and (b) at $E_{cm} = 133$ GeV from Monte Carlo models.

experimental systematic error.

The fitting procedure is essentially the same as that described in the previous ALEPH analysis [15], the main differences being the following:

- The fits presented here use a large fit range: $1.2 < L < 7.6$.
- An improved QCD prediction for the distribution is used [20].
- The values are obtained using hadronization corrections based on ARIADNE, since this yielded a significantly lower χ^2 value at $E_{cm} = 91.2$ GeV. Hadronization uncertainties are derived by considering the difference in α_s when using the PYTHIA and HERWIG models to derive the corrections. (As in Ref. [21], the hadronization correction was applied by means of a folding matrix.)
- Bin-to-bin correlations, which are important because of the large bins, are taken into account by assuming a multinomial distribution. The covariance matrix used in the fit is thus $V_{ij} = p_i(\delta_{ij} - p_j)/(N\Delta L)$, where $N = 299$ is the total number of events, $\Delta L = 0.8$ is the bin width, and p_i is the theoretical probability for an event to be in bin i.

Fit results for $E_{cm} = 91$ and 133 GeV are shown in Fig. 9, where the combination of the resummed and fixed order parts of the QCD prediction is based on the R matching scheme [15]. The quality of the fit is seen to be good at 133 GeV. Because of the smaller errors at 91.2 GeV, however, discrepancies between the fitted distribution and the data become evident. The χ^2 values for the fits shown are 55.2 (91.2 GeV) and 7.3 (133 GeV) for 7 degrees of freedom. Using the $\ln R$ matching scheme gives almost exactly the same goodness-of-fit, with $\chi^2 = 55.2$ (91.2 GeV) and $\chi^2 = 7.1$ (133 GeV). As done in Ref. [15], the nominal value of α_s is determined by averaging the results of the two matching schemes at a value of the renormalization scale $\mu = E_{cm}$. This gives

$$\alpha_s(91.2\,\mathrm{GeV}) = 0.1200 \pm 0.0003(stat.) \pm 0.0023(sys.) \pm 0.0016(hadr.) \pm 0.0066(theo.)\,,$$

$$\alpha_s(133\,\mathrm{GeV}) = 0.1189 \pm 0.0043(stat.) \pm 0.0025(sys.) \pm 0.0008(hadr.) \pm 0.0067(theo.)\,.$$

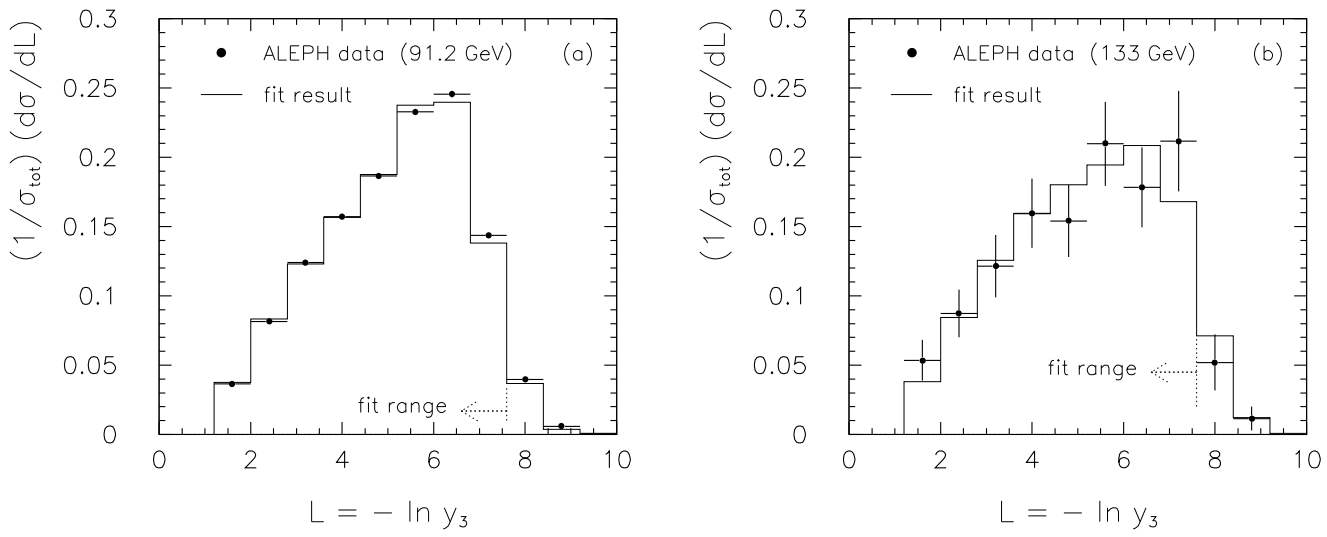

Figure 9: Fit of QCD prediction to the distribution of $L = -\ln y_3$ (a) at $E_{cm} = 91.2$ GeV and (b) at $E_{cm} = 133$ GeV.

By varying the analysis procedure as described in Section 3, an uncertainty in $\alpha_s(133\,\mathrm{GeV})$ of 0.0011 is obtained. This is (conservatively) added in quadrature with the experimental systematic error of 0.0023 obtained at 91.2 GeV, which is dominated by the change in α_s when determining y_3 using charged particles only. This component of the error is expected to be highly correlated between the two energies.

The theoretical errors reflect the uncertainty in the perturbative QCD formula due to missing higher order terms. As in the previous ALEPH analysis this was determined by varying the renormalization scale μ in the range $-1 < \ln \mu^2/s < 1$ using both the R and $\ln R$ matching schemes and taking the largest deviation from the nominal value. As expected, the theoretical error is found to be highly correlated between the two energy points, and therefore does not play a significant role in the observation of the running of α_s.

Because of the large fit range used, the value of α_s determined at $E_{cm} = 91.2$ GeV has a larger total uncertainty than that published in Ref. [15], and is presented here only for purposes of investigating the energy dependence of α_s. The difference in the two α_s values is

$$\alpha_s(91.2\,\mathrm{GeV}) - \alpha_s(133\,\mathrm{GeV}) = 0.0011 \pm 0.0043\,(stat.) \pm 0.0011\,(sys.) \pm 0.0018\,(hadr.)\,.$$

The component of the experimental systematic error of 0.0023 determined at 91.2 GeV as well as the theoretical uncertainty are not included here since they are highly correlated between the two energy points. The change in α_s is smaller than but consistent with the expected change of 0.007.

The fitted QCD prediction in Fig. 10 gives $\chi^2 = 1.33$ for one degree of freedom. For the fit, the errors were taken to be the quadratic sums of statistical and hadronization uncertainties, as well as the component of the experimental systematic uncertainty of 0.0011 determined at 133 GeV. If the component of the experimental systematic error of 0.0023 determined at 91.2 GeV were to be assumed to be uncorrelated with the corresponding component at 133 GeV, one would obtain $\chi^2 = 0.94$.

This slightly higher than expected value of $\alpha_s(133\,\mathrm{GeV})$ is related to the larger than expected value of $\langle 1 - T \rangle$ seen in Fig. 6. In contrast to this, the measurement by the L3 Collaboration of

$\alpha_s(133\,\mathrm{GeV}) = 0.107 \pm 0.005\,(exp.) \pm 0.006\,(theor.)$ [11], which is based on a similar technique, is somewhat lower than the QCD prediction, as is their measured value of $\langle 1 - T \rangle$.

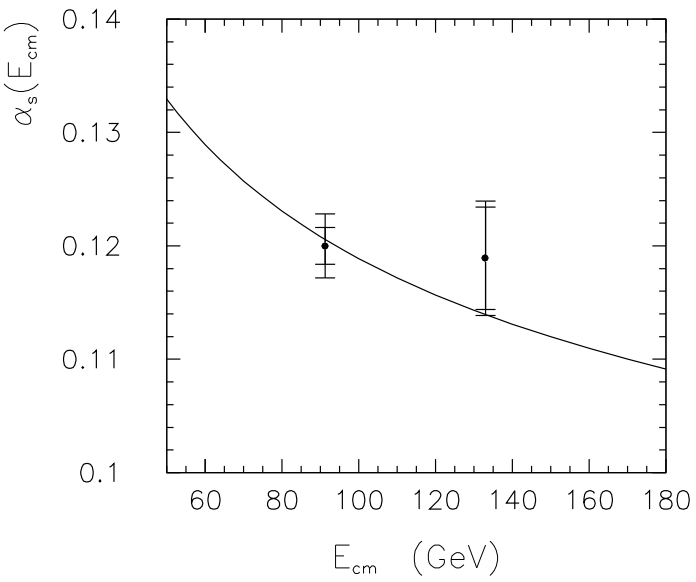

Figure 10: Values of $\alpha_s(E_{cm})$ determined at $E_{cm} = 91.2$ and 133 GeV along with the fitted QCD prediction. The inner error bars are the quadratic sums of statistical and hadronization errors, as well as the uncorrelated component of the experimental systematic error (0.0011) at 133 GeV. The outer error bars include the entire experimental systematic uncertainty.

7 Conclusions

Properties of hadronic final states produced in e^+e^- annihilation at $E_{cm} = 130$ and 136 GeV have been measured based on a data sample of 5.7 pb^{-1} collected by the ALEPH detector at LEP. The mean multiplicity of charged particles N_{ch} is found to be

$$N_{ch}(133\,\mathrm{GeV}) = 24.13 \pm 0.43\,(stat.) \pm 0.34\,(sys.)$$

and the peak position of the inclusive distribution of $\xi = -\ln x_p$ ($x_p = p/p_{beam}$) to be

$$\xi^*(133\,\mathrm{GeV}) = 3.834 \pm 0.038\,(stat.) \pm 0.029\,(sys.)\,.$$

By comparing with lower energy measurements the energy evolution of these two quantities is found to be in agreement with that predicted by QCD. Only small discrepancies with the predictions of QCD-based models are observed, e.g. more particles are seen at low momenta and at low rapidity than predicted.

Measurements of jet rates and event-shape distributions show good general agreement with QCD expectations. The mean thrust at $E_{cm} = 133$ GeV is measured to be

$$\langle 1 - T \rangle = 0.0666 \pm 0.0060\,(stat.) \pm 0.0030\,(sys.)\,.$$

The strong coupling constant is determined from the differential two-jet rate (distribution of $-\ln y_3$) to be

$$\alpha_s(133\,\mathrm{GeV}) = 0.1189 \pm 0.0043(stat.) \pm 0.0025(sys.) \pm 0.0008(hadr.) \pm 0.0067(theo.)\,.$$

By comparing with the corresponding value determined at $E_{cm} = 91.2$ GeV, the expected energy evolution of α_s is confirmed with a χ^2 of 1.33 for one degree of freedom. The change in α_s between the two energies is

$$\alpha_s(91.2\,\mathrm{GeV}) - \alpha_s(133\,\mathrm{GeV}) = 0.0011 \pm 0.0043\,(stat.) \pm 0.0011\,(sys.) \pm 0.0018\,(hadr.)\,.$$

Higher statistics measurements at LEP II will allow a more thorough examination of the energy dependence of all of these quantities.

Acknowledgements

We are grateful to Mike Seymour for providing the preliminary version 5.8d of the HERWIG model. We wish to thank our colleagues from the accelerator divisions for the successful operation of LEP, and we congratulate them on the upgrade to higher energy. We are indebted to the engineers and technicians in all our institutions for their contribution to the good performance of ALEPH. Those of us from non-member countries thank CERN for its hospitality.

References

[1] D. Decamp et al., ALEPH Collab., Nucl. Instr. Meth. **A294** (1990) 121

[2] D. Decamp et al., ALEPH Collab., Phys. Rep. **216** (1992) 253; D. Buskulic et al., ALEPH Collab., Nucl. Instr. Meth. **A360** (1995) 481.

[3] D. Buskulic et al., ALEPH Collab., Z. Phys. **C55** (1992) 209.

[4] T. Sjöstrand, Computer Physics Commun. **82** (1994) 74.

[5] G. Marchesini, B.R. Webber, G. Abbiendi, I.G. Knowles, M.H. Seymour, and L. Stanco, Computer Physics Commun. **67** (1992) 465; version 5.8d provided by M.H. Seymour.

[6] W. Bartel et al., JADE Collab., Z. Phys. **C33** (1986) 23; S. Bethke et al., JADE Collab., Phys. Lett. **B213** (1988) 235.

[7] L. Lönnblad, Computer Physics Commun. **71** (1992) 15.

[8] D. Buskulic et al., ALEPH Collab., *Studies of Quantum Chromodynamics with the* ALEPH *Detector*, to be published.

[9] D. Decamp et al., ALEPH Collab., Z. Phys. **C53** (1992) 21.

[10] P. Abreu et al., DELPHI Collab., *Charged Particle Multiplicity in* e^+e^- *Interactions at* $\sqrt{s} = 130$ *GeV*, CERN-PPE/96-05, 1996.

[11] M. Acciarri et al., L3 Collab., *Studies of Hadronic Event Structure and* α_s *Determination at* $\sqrt{s} = 130, 136$ *GeV*, CERN-PPE/95-192, 1995.

[12] Y.K. Li et al., AMY Collab., Phys. Rev. **D41** (1990) 2675;
H.W. Zheng et al., AMY Collab., Phys. Rev. **D42** (1990) 737:
W. Braunschweig et al., TASSO Collab., Z. Phys. **C45** (1989) 193;
W. Bartel et al., JADE Collab., Z. Phys. **C20** (1983) 187;
M. Derrick et al., HRS Collab., Phys. Rev. **D34** (1986) 3304.

[13] W. Braunschweig et al., TASSO Collab., Z. Phys. **C47** (1990) 187.

[14] Yu.L. Dokshitzer, V.A. Khoze, A.H. Mueller and S.I. Troyan, *Basics of Perturbative QCD*, Editions Frontières, Gif-sur-Yvette, 1991.

[15] D. Decamp et al., ALEPH Collab., Phys. Lett. **B284** (1992) 163.

[16] S. Catani, Yu.L. Dokshitzer, M. Olsson, G. Turnock and B.R. Webber, *Phys. Lett.* **B269** (1991) 432.

[17] Proceedings of the Durham Workshop, W.J. Stirling, *J. Phys.* **G**: *Nucl. Part. Phys.* **17** (1991) 1567;
N. Brown and W.J. Stirling, Phys. Lett. **B252** (1990) 657;
S. Bethke, Z. Kunszt, D.E. Soper and W.J. Stirling, Nucl. Phys. **B370** (1992) 310.

[18] D. Buskulic et al., ALEPH Collab., *Four-Jet Final State Production in e^+e^- Collisions at Centre-of-Mass Energies between 130 and 140 GeV*, to be published.

[19] Yu.L. Dokshitzer, G. Marchesini, B.R. Webber, *Dispersive Approach to Power-Behaved Contributions in QCD Hard Processes*, CERN-TH/95-281, 1995.

[20] G. Dissertori and M. Schmelling, Phys. Lett. **B361** (1995) 167.

[21] D. Decamp et al., ALEPH Collab., Phys. Lett. **B255** (1991) 623.